



Effect of metal fluorides on the corrosion of structural materials in molten LiF-NaF-KF

Krishna Moorthi Sankar, Preet M. Singh*

School of Materials Science and Engineering, Georgia Institute of Technology, Atlanta, GA, USA



ARTICLE INFO

Keywords:
Molten Salt
Corrosion
FLiNaK
Metal Fluorides
Impurity Effects

ABSTRACT

The corrosion of structural materials in molten fluoride salts is predominantly caused by the presence of impurities in the salt. This study focuses on understanding the corrosion behavior of selected alloys in molten FLiNaK salt with addition of similar quantities of metal fluoride impurities such as CrF₂, CrF₃, FeF₂, FeF₃, and NiF₂. The results show that the presence of selected metal fluoride impurities increases the extent of corrosion of the selected alloys in molten FLiNaK salt, with the exact effect depending on the thermodynamic stability of the fluoride impurity added as well as the composition of the structural alloy studied.

1. Introduction

Molten fluoride salts such as LiF-BeF₂ (FLiBe) and LiF-NaF-KF (46.5–11.5–42 mol%, also called FLiNaK) are being considered as potential heat transfer fluids and coolants in Molten Salt Nuclear Reactors (MSR) and Concentrated Solar Power Plant (CSP) designs due to their excellent thermal conductivity, heat transfer properties, and small neutron cross-section [1,2]. Fluoride-cooled High-temperature Reactors (FHRs) are MSR designs in which the fuel is inserted as solid fuel elements with the molten salt acting as coolant in the primary and secondary coolant loops [3].

FLiNaK is a major candidate for application as a coolant in FHRs, especially in the secondary coolant loops. However, the corrosion of structural materials used for construction of FHRs and CSPs in the molten FLiNaK salt, especially at higher temperatures required for FHRs, is a major design concern [4]. Under equilibrium conditions, the salt components of FLiNaK (Li, Na, and K) all form thermodynamically more stable fluorides as compared to alloying elements in structural materials of interest, as shown in Fig. 1. The Gibbs Free Energy values in Fig. 1 have been obtained using HSC Chemistry® 9.0 Thermodynamic software. However, the presence of impurities can upset this equilibrium and can lead to the selective dissolution of more active alloying elements from the structural materials [5–8]. This selective dissolution can lead to formation of metal fluorides of alloying elements in the salt, which can further change the properties of the salt as well as the corrosion behavior of materials in that salt [5,9].

Many candidate alloys have been considered for application as

structural materials for the construction of FHRs and CSPs [10]. The most commonly considered material classes for these applications are Nickel-based alloys such as Hastelloy N and Haynes 244 for their high corrosion resistance, Austenitic Stainless Steels such as 316H for their high temperature strength and low cost, or Fe-Ni-Cr alloys such as Incoloy 800H for a combination of these properties [10]. Most of these materials have a high content of Cr and Ni or Fe along with other alloying elements such as Mo and W. As such, given the energy of formation of fluorides, the most likely metal fluorides that may be present in FHR or CSP conditions are fluorides of Cr and Fe such as CrF₂, CrF₃, FeF₂, and FeF₃. If Ni-based superalloys are used as structural materials, the presence of NiF₂ is also likely due to the dissolution of NiO passive layer in the molten FLiNaK. Presence of any impurities such as moisture, actinides, oxides etc. can all lead to the presence of these impurities in the molten salt [5,11,12]. Due to the likelihood of presence of these metal fluorides in molten salt in small quantities at some point in FHR or CSP life cycle, it is important to understand the effect of their presence on the corrosion of structural materials in the molten fluoride salts.

The effect of some of these metal fluorides on the degradation of various candidate alloys in molten fluoride salts have been studied in the past. Pavlik et al. studied the effect of presence of various quantities of CrF₃, FeF₂, FeF₃, and NiF₂ on the corrosion of Incoloy 800H in molten FLiNaK salt and observed that the degradation behavior showed a parabolic variation with quantity of fluoride added for each of these fluorides [13]. Wang et al. studied the effect of 0.09 and 0.18 mol% CrF₃ on the corrosion of GH3535 and found that the presence of CrF₃ led to increased corrosion attack in molten FLiNaK salt [14]. Yin et al. arrived

* Corresponding author.

E-mail address: preet.singh@mse.gatech.edu (P.M. Singh).

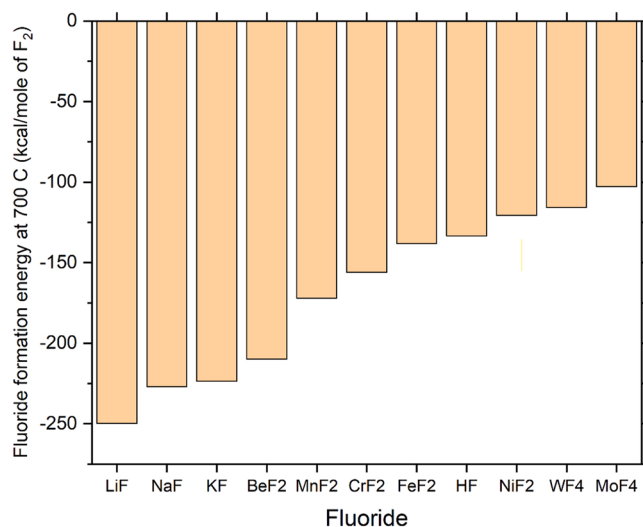


Fig. 1. Gibbs free energy of formation of different fluorides in kcal/mole of F₂ at 700 °C as calculated using HSC Chemistry® 9.0 thermodynamic software.

Table 1
Compositions (in wt%) of Hastelloy N and SS316H, average of three samples measured by XRF.

Alloy	Cr	Fe	Ni	Mo	Mn	Co	Si
Hastelloy N	7.64	4.38	71.36	15.86	0.57	0	0
SS316H	16.72	68.72	10.28	2.03	1.46	0.25	0.14

at the same conclusion after studying the effect of 0.4 wt% (0.16 mol%) CrF₃ on the corrosion of Hastelloy N and SS316L in molten FLiNaK salt and observed that SS316L performed worse than Hastelloy N under these conditions [15]. Doniger et al. showed that presence of CrF₃ and FeF₃ in molten FLiBe can lead to increased corrosion by Cr depletion in SS316H, and that they can be detected by application of cyclic voltammetry [16]. Ai et al. added FeF₃ in various quantities to molten

FLiNaK salt and found that the corrosion of GH3535 increased with the quantity of added FeF₃ and that there was a deposition of Fe on the surface of the alloy after exposure to higher quantities of FeF₃[17].

In most commercial or research designs of FHRs, the candidate alloys considered are usually Hastelloy N or its equivalents such as GH3535, which were specifically developed for MSR applications [18] or SS316H, which is ASME code certified for high temperature applications [19]. However, the effect of presence of different metal fluorides on the corrosion of these alloys have not been comparably studied. While there are certain studies on the effect of a particular fluoride on the corrosion of these specific alloys [14,16], the effect of comparable quantities of different metal fluorides on these alloys have not been studied. Pavlik et al. found that Incoloy 800 H showed a corrosion behavior that increased with added metal fluorides as CrF₃ < FeF₂ < FeF₃ < NiF₂ for comparable quantities of fluorides [13]. However, as the mixed Fe-Cr-Ni alloy Incoloy 800 H is a very different alloy in terms of composition from either the austenitic stainless steel SS316H or the Ni-based Hastelloy N, whether these materials will behave in a similar manner has to be studied and confirmed.

In this study, the effects of presence of similar quantities of various metal fluorides of Cr, Fe, and Ni that are more likely to be present in FHR and CSP conditions on the corrosion of austenitic stainless steel SS316H and nickel-based alloy Hastelloy N in molten FLiNaK salt have been studied. The depth of corrosion attack on the alloys exposed to molten FLiNaK, with and without the addition of various metal fluorides has been compared to understand the effect of selected metal fluorides on the corrosion behavior of these alloys. Our results demonstrate that different metal fluorides have similar effects on the mode of corrosion of alloys while the extent is largely determined by both the thermodynamic stability of the fluoride added as well as the composition of the structural alloy studied.

2. Materials and methods

Nickel based alloy Hastelloy N (manufactured by Haynes International) and Austenitic Stainless Steel 316H (manufactured by Sandmeyer Steel) were chosen as the materials for studying the effects that presence of metal fluorides can have on their corrosion. The average

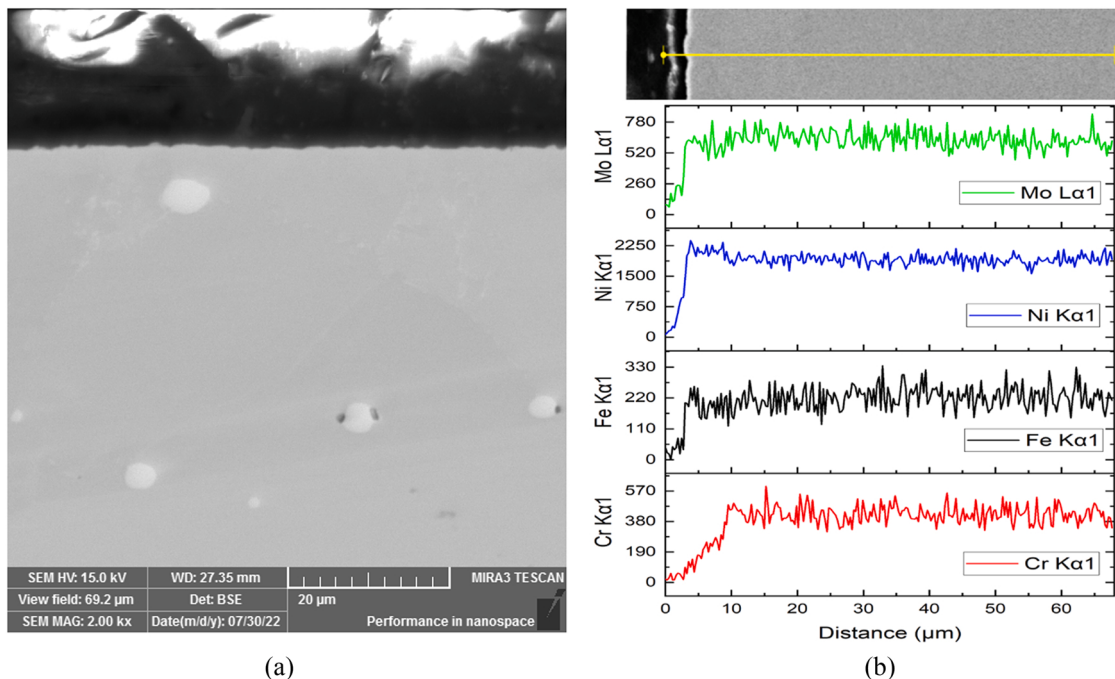


Fig. 2. (a) SEM image and (b) EDS line scan of cross-section of Hastelloy N sample exposed to baseline FLiNaK salt.

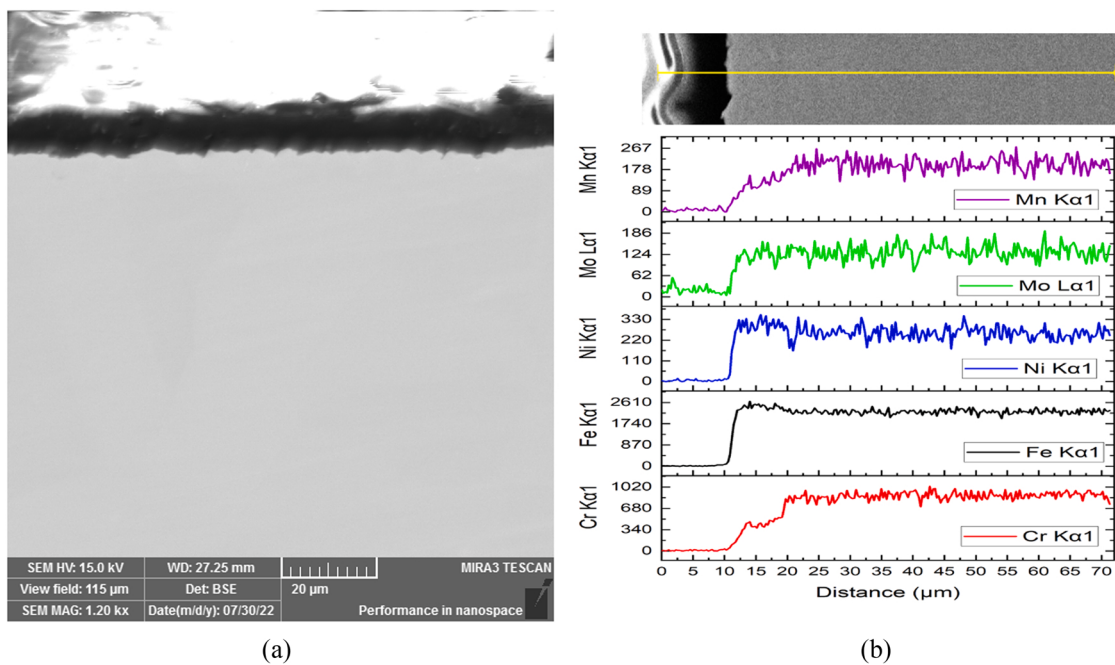


Fig. 3. (a) SEM image and (b) EDS line scan of cross-section of SS316H sample exposed to baseline FLiNaK salt.

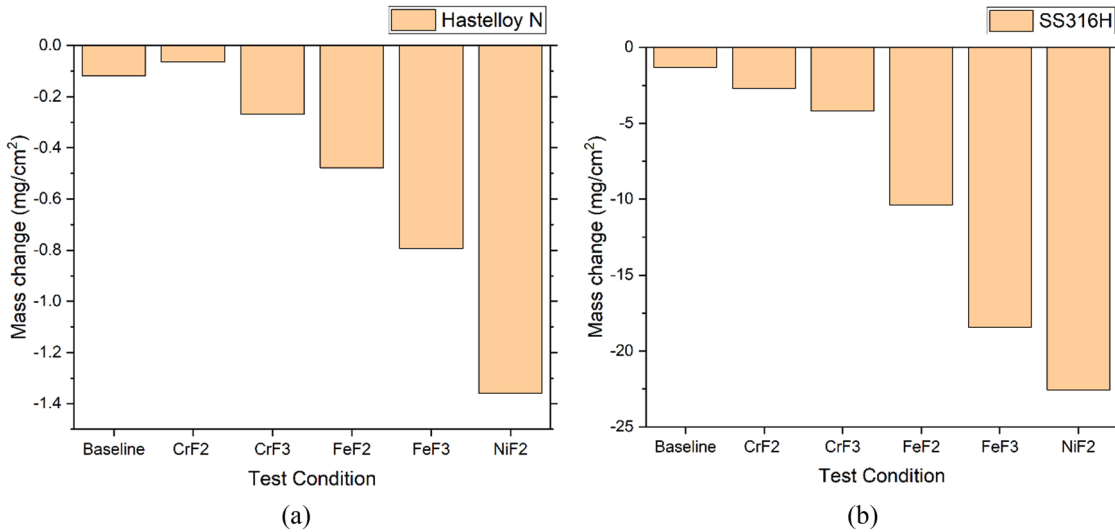


Fig. 4. Mass change values for (a) Hastelloy N and (b) SS316H samples exposed to molten FLiNaK with and without added metal fluorides.

compositions of these alloys as determined using X-Ray Fluorescence Spectroscopy (XRF, Oxford X-MET 8000 Optimum) are given in Table 1.

The alloy samples and the FLiNaK salt were prepared in the same manner as described in previous papers [20,21]. The concentration of Fe in the purified FLiNaK salt was found to be 160 μg/g and all other cationic impurities such as Ni, Cr, Mo, Mn etc. in the salt were found to be below detection limits (10–20 μg/g depending on the element) using ICP-MS. All tests were performed in a glove box with oxygen and moisture levels maintained at < 2 ppm. The pure Ni crucibles containing the samples were filled with 10 g molten fluoride salt mixture with known amounts of FLiNaK and 0.2 mol.% each of CrF₂ (>99 % Pure, Synquest Labs), CrF₃ (>99 % Pure, Synquest Labs), FeF₂ (>99 % Pure, Strem Chemicals), FeF₃ (>99 % Pure, Millipore Sigma), or NiF₂ (>99 % Pure, ThermoScientific) and placed in a crucible rack inserted into a cylindrical furnace in the glove box. Exposure tests were performed at 700 °C for 100 h. After the exposure tests, the samples were taken out,

cleaned, and characterized for the corrosion mode and extent by using XRF, X-Ray Diffractometry (XRD), Scanning Electron Microscopy (SEM), and Energy Dispersive X-Ray Spectroscopy (EDS) as in our previous study [21].

3. Results and discussion

To study the effect of presence of various metal fluorides in molten FLiNaK salt on the corrosion of structural materials in the salt, it is necessary to establish a baseline of expected corrosion of these materials in molten FLiNaK salt without any added impurities. In this study, a specimen of both Hastelloy N and SS316H were separately exposed to molten FLiNaK salt for 100 h at 700 °C. The alloys were cross sectioned after the test and the SEM images and EDS line scans of these cross-sections are given in Figs. 2 and 3 respectively. As it can be observed from the EDS line scans, the mode of corrosion in both of these alloys is

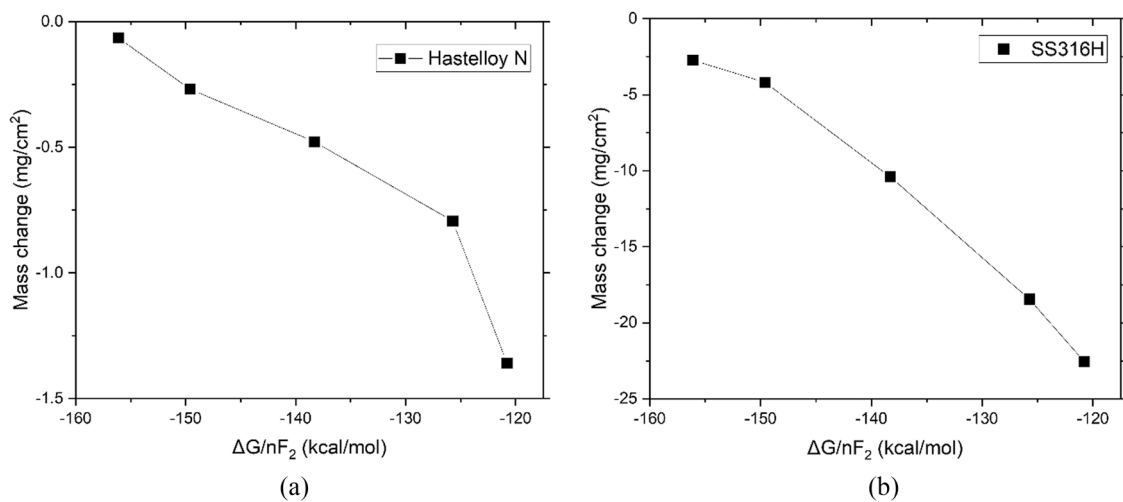
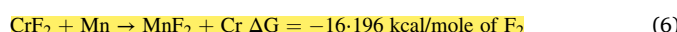
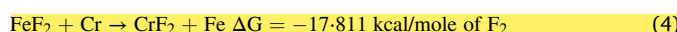
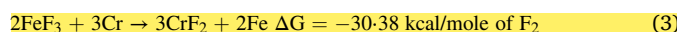
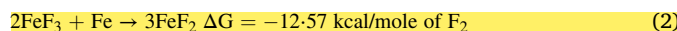
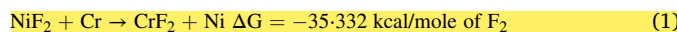


Fig. 5. Correlation between mass change and ΔG of fluoride formation (from Fig. 1) for (a) Hastelloy N and (b) SS316H samples exposed to molten FLiNaK with various added metal fluorides.

the selective depletion of active elements like Cr and Mn from the surface. The extent of attack in terms of this selective dissolution in these baseline samples is about 8–10 μm . These results for this particular batch of salt are very similar to the baselines established in our previous study [21].

To understand the effect of different metal fluorides on the corrosion of selected structural materials in molten FLiNaK salt, CrF_2 , CrF_3 , FeF_2 , FeF_3 , and NiF_2 were added at a concentration of 0.2 mol% each in purified molten FLiNaK salt. The amount was fixed to 0.2 mol% for all tested impurities in this study to understand and compare their relative effect on the corrosion of structural alloys. It is unlikely that concentration of these impurities would be present at a higher concentration than 0.2 mol% during FHR or CSP operation. The same mol% values were chosen for addition of all metal fluorides to enable comparison between the corrosion results from each of these metal fluoride additions. The expected effect with the addition of selected metal fluorides is that they lead to formation of metal fluorides of more active alloying elements through disproportionation reactions, which will lead to selective dissolution of these elements from the alloy, leading to degradation of the alloy. The Gibbs Free Energies for the various disproportionation and fluorination reactions that can occur as calculated by HSC Chemistry® 9.0 are:



The mass change values for SS316H and Hastelloy N samples after exposure to molten FLiNaK, and molten FLiNaK with added metal fluorides, for 100 h at 700 °C is given in Fig. 4. This data shows that, for SS316H, the mass change increases significantly with the addition of metal fluorides, where the metal fluorides with more positive energy of formation such as NiF_2 have a higher effect. This is similar to the effect observed in previous works with multiple metal fluorides [13] as well as with metal oxides [21]. As mentioned earlier, the addition of FeF_2 , NiF_2 etc. can lead to formation of CrF_2 due to disproportionation reactions, which can lead to selective leaching of Cr and mass loss. The less stable fluorides such as NiF_2 will more readily react with Cr and Mn to form CrF_2 and MnF_2 leading to a faster kinetics of corrosion. For Hastelloy N,

on the other hand, the overall effect is much less noticeable than for SS316H. It was observed that the addition of CrF_2 to Hastelloy N led to lower mass loss as compared to the baseline sample, indicating the possibility of formation of corrosion products or intermetallics at the surface which might be impeding the Cr diffusion or adding to the overall mass of the test sample. The addition of other metal fluorides also led to an increased mass loss as compared to the baseline sample, however, the effect was less than that for SS316H. This change from SS316H samples could be due to the limited amount of active elements such as Cr, Mn, and Fe available for disproportionation reaction in Hastelloy N as compared to SS316H.

To further understand the effect of metal fluorides, the variation in mass loss for the specimens with the change in energy of formation of the added fluoride is given in Fig. 5. The change in energy of formation of the added fluoride is taken as the values from Fig. 1 for CrF_2 , CrF_3 , FeF_2 , FeF_3 , and NiF_2 . It was observed that, for SS316H, the change in mass loss is exponential with the decrease in the energy of formation of a given metal fluoride, whereas for Hastelloy N, this change is nearly linear with the decrease in the energy of formation. The possible reasons for this change may be the difference in the amount of disproportionation reaction that can take place in a Fe-based alloy as opposed to a Ni-based alloy, as well as due to the differences in the mode of attack for the two alloys. It has been demonstrated repeatedly in literature that, in the presence of impurities in molten FLiNaK salt, Hastelloy N is more likely to undergo bulk attack, whereas SS316H is more likely to undergo intergranular attack [20,22]. The presence of a distinct, high-energy path for the diffusion of alloying elements can lead to higher corrosion attack and a higher mass loss. In addition, we can observe from the energy of fluoride formation that Fe forms a more stable fluoride than Ni. As a result, metal fluorides such as FeF_3 and NiF_2 , could lead to the formation of FeF_2 from Fe in SS316H, but not NiF_2 from Ni in Hastelloy N. The presence of NiF_2 in FLiNaK does lead to a much higher mass loss for Hastelloy N than a linear relation would suggest. It is possible that the presence of a metal fluoride impurity of a more noble metal such as Pt, that is less stable than NiF_2 could lead to a similar exponential effect of mass loss vs energy of fluoride formation on Hastelloy N as well. However, the presence of such metal fluorides in FHRs or CSPs is very unlikely, and hence was not explored in this work.

The XRD results for SS316H samples tested with and without different metal fluorides, as well as for an untested 316H sample, are given in Fig. 6. The SS316H sample tested in baseline FLiNaK, without added impurities, showed peaks corresponding to both ferrite/martensite and austenite iron, unlike the untested sample which only shows peaks corresponding to austenite iron. As reported in our previous

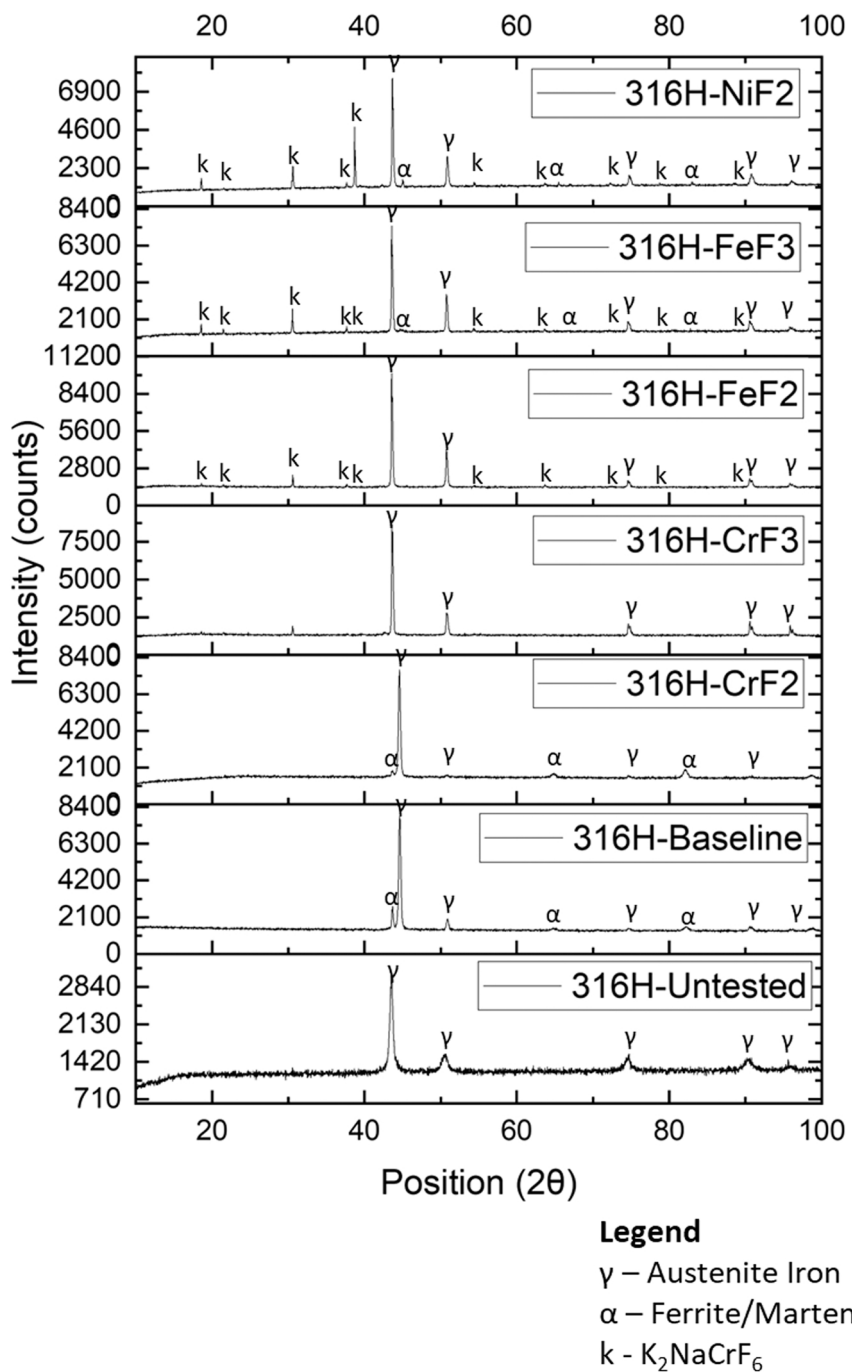


Fig. 6. XRD peaks for SS316H samples before and after being exposed to molten FLiNaK salt with or without added metal fluorides.

work, this is mainly due to the leaching of Cr and Mn, leading to reduced stability for FCC austenite which results in the formation of BCC ferrite or BCT martensite [21,23,24]. Even though Cr is typically a ferrite stabilizer, it has been shown thermodynamically by Butler et al. [24] and Chan [23] that leaching of Cr and Mn from austenitic stainless steels leads to formation of BCT martensite phases. Alongside the loss of Mn, which is an austenite stabilizer, this selective leaching also leads to the selective enrichment of Mo, which is a ferrite stabilizer, at the surface. These changes of composition at the surface of austenitic stainless steels are postulated to lead to stabilization of ferrite or martensite structure at the surface [24]. In this study, this peak has been marked as ferrite/martensite iron in Fig. 6 as it is difficult to distinguish between these phases with the XRD.

Similar results are observed for the sample exposed to molten FLiNaK

with added CrF₂. However, the sample exposed to molten FLiNaK with added CrF₃ does not display peaks corresponding to BCC ferrite or BCT martensite, which is presumably due to the intergranular nature of the attack which does not cause Cr depletion from the surface and does not lead to bulk Ferrite formation at the surface. The SS316H sample tested with addition of FeF₂ shows peaks corresponding to FCC as well as several other peaks corresponding to K₂NaCrF₆ [25,26] whereas the samples exposed to FLiNaK with added FeF₃ and NiF₂ show these peaks in addition to the peaks corresponding to BCC/BCT phases. K₂NaCrF₆ has been shown to form on the surface of austenitic stainless steels when excess fluorine or metal fluorides are present [26,27]. The formation of this compound is also known to occur simultaneously with large selective depletion of Cr and Fe from the alloy surface [26].

The SEM images and EDS maps of cross-sections of SS316H samples

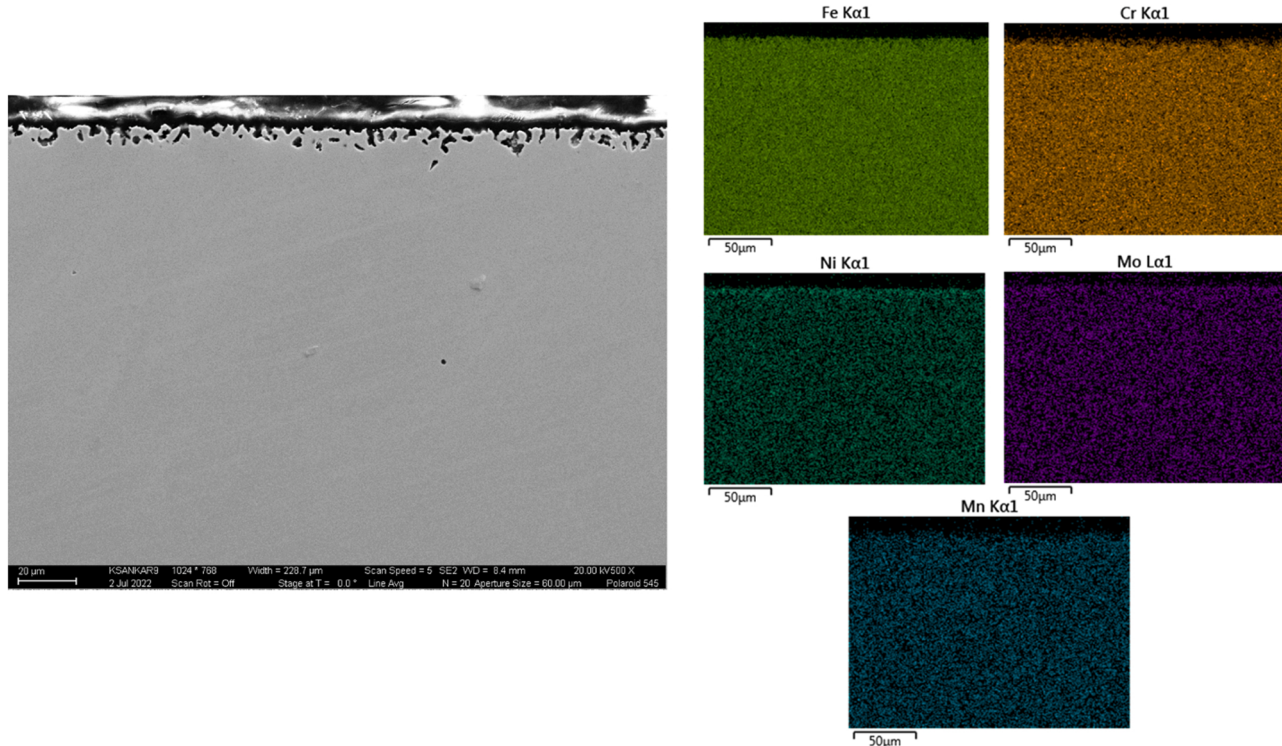


Fig. 7. SEM image and EDS maps of cross-section of SS316H sample exposed to FLiNaK salt with added 0.2 mol% CrF₂.

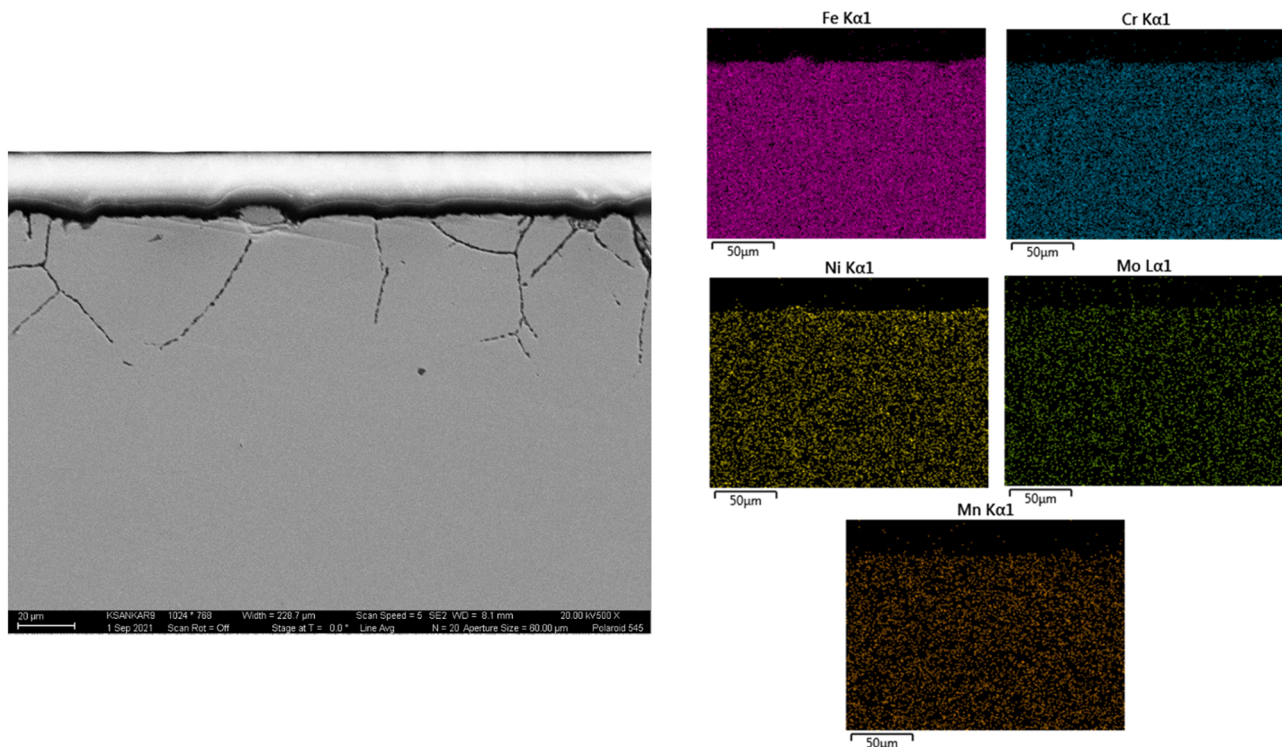


Fig. 8. SEM image and EDS maps of cross-section of SS316H sample exposed to FLiNaK salt with added 0.2 mol% CrF₃.

exposed to molten FLiNaK with added CrF₂, CrF₃, FeF₂, FeF₃, and NiF₂ are given in Figs. 7–11, respectively. Please note that, unlike with the other results reported in this study, the EDS results reported here are maps and not line scans. This is because of the intergranular nature of the attack, which cannot be effectively captured by line scans, whereas

the selective leaching observed in the other samples in this study cannot be observed very well with EDS maps. Similar to the mass change values in Fig. 4, we observed an increase in the extent of intergranular attack in the SS316H samples with the decrease in stability of the metal fluoride added. Addition of CrF₂ in Fig. 7 led to an attack that is about 10 μ m

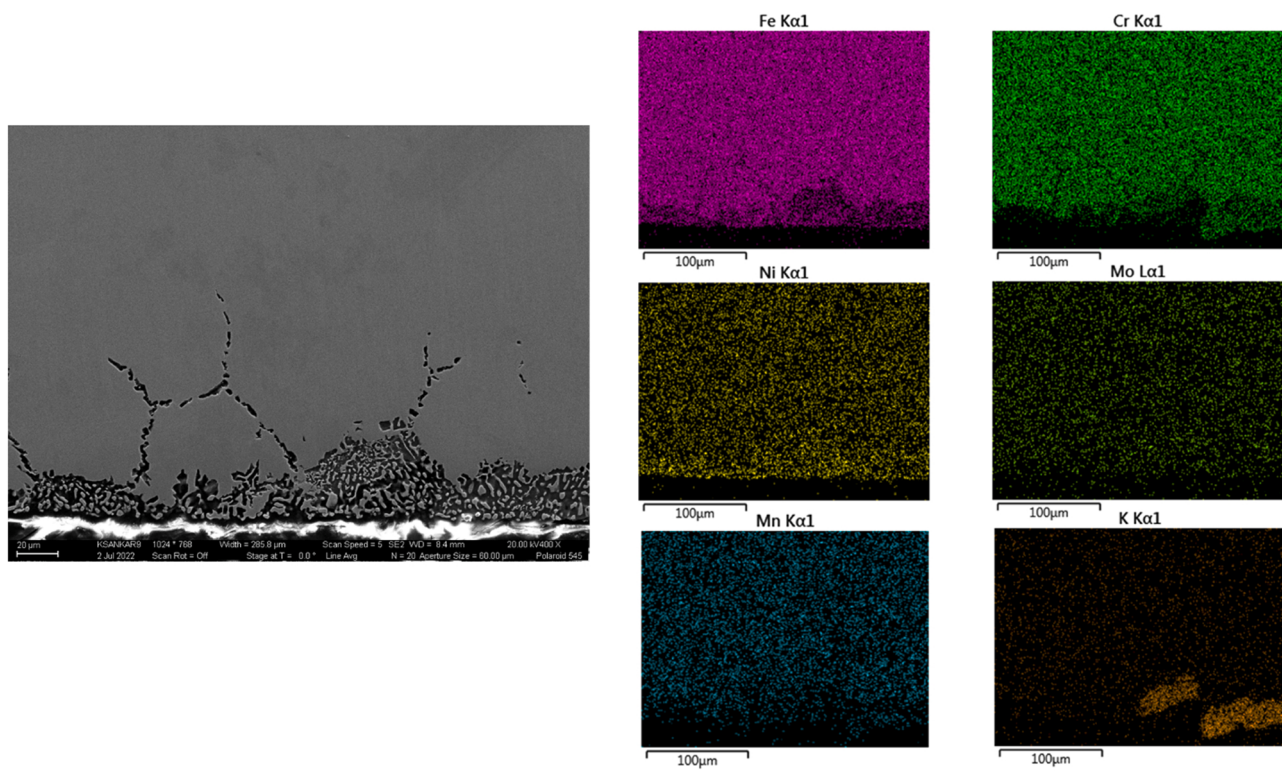


Fig. 9. SEM image and EDS maps of cross-section of SS316H sample exposed to FLiNaK salt with added 0.2 mol% FeF₂.

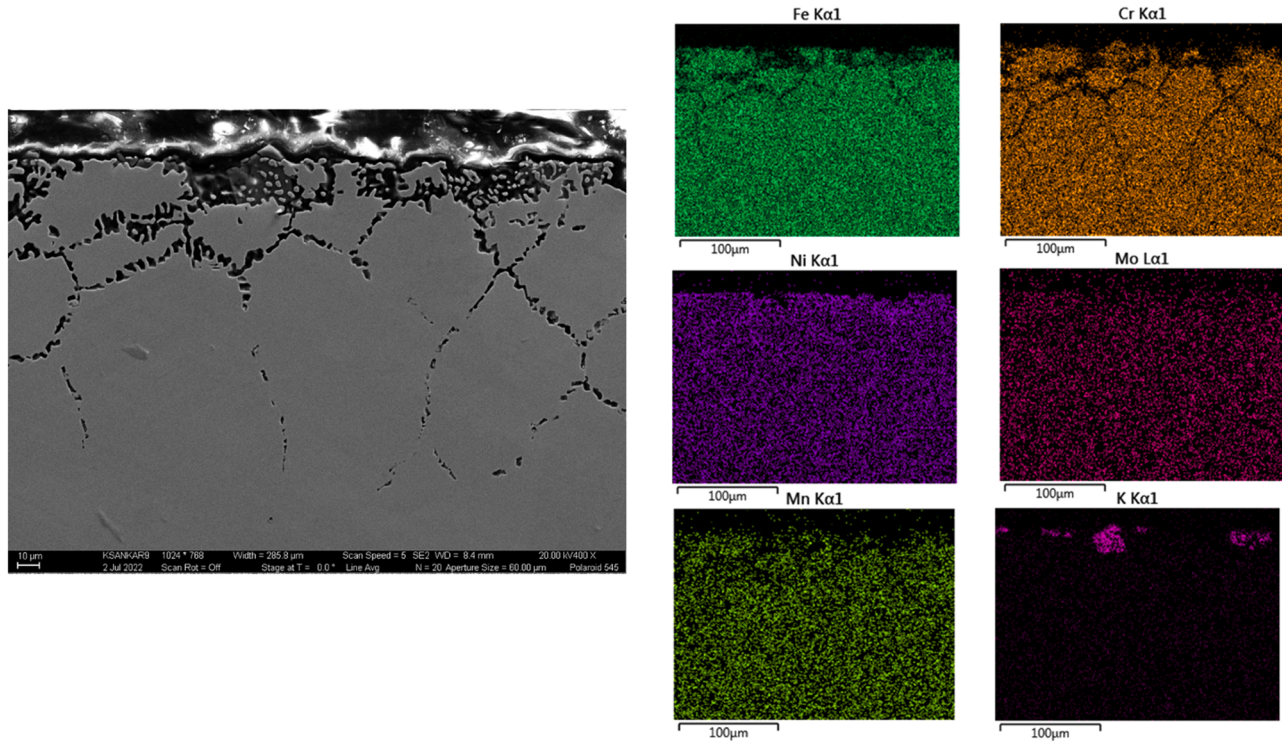


Fig. 10. SEM image and EDS maps of cross-section of SS316H sample exposed to FLiNaK salt with added 0.2 mol% FeF₃.

deep while the addition of NiF₂ in Fig. 11 resulted in about 200 μm deep attack. It can be observed that the extent of intergranular attack increases from CrF₂ (10 μm) to CrF₃ (50 μm) to FeF₂ (100 μm) to FeF₃ (180 μm) to NiF₂ (200 μm). Certain areas in the samples exposed to FeF₂, FeF₃, and NiF₂ also show non-uniform growth of structures at the

surface, which can be identified from the EDS maps as K₂NaCrF₆ structures in Figs. 9–11. These images demonstrate that the K₂NaCrF₆ formation in SS316H is non-uniform in nature, with certain areas not showing the presence of this compound at all while certain areas show a large concentration of this compound. This is in confirmation with

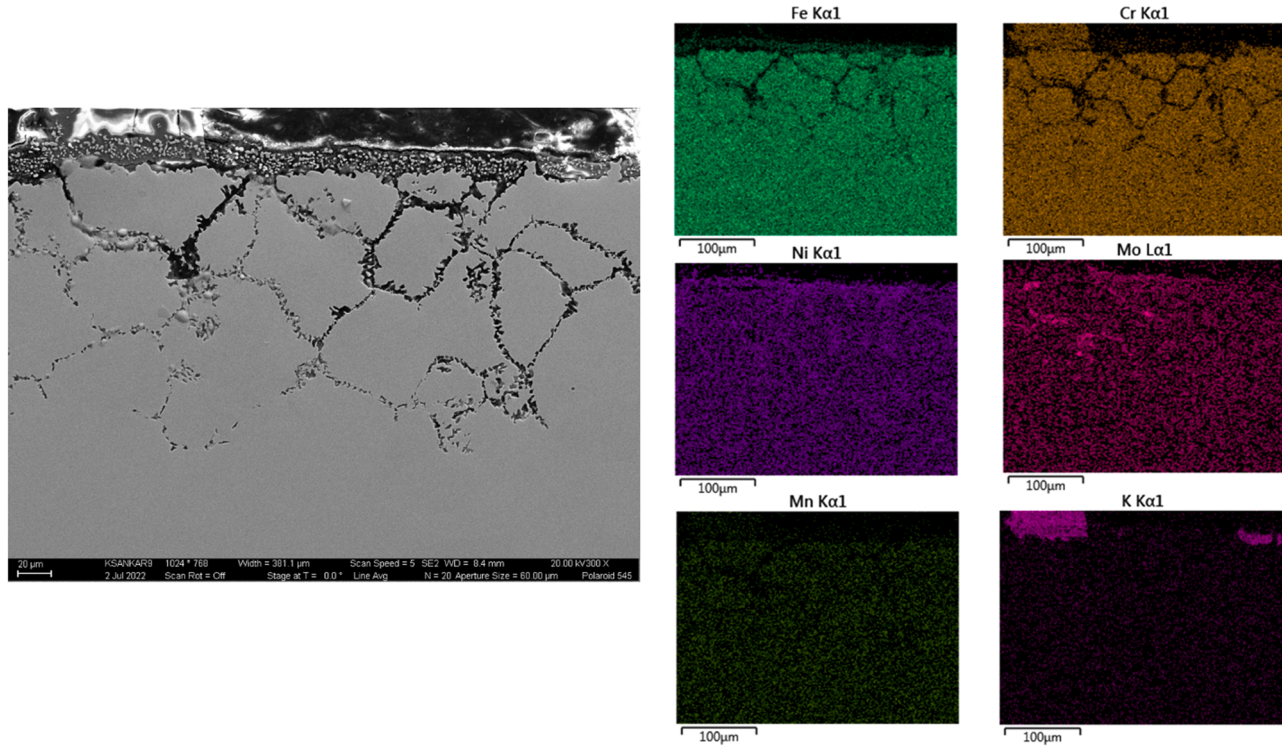


Fig. 11. SEM image and EDS maps of cross-section of SS316H sample exposed to FLiNaK salt with added 0.2 mol% NiF₂.

previous studies [26,28] which showed that K₂NaCrF₆ formed in pockets. While the exact properties of this compound are not known, the non-metallic nature of this compound suggests that it is likely to have a lower strength and structural stability.

The XRD results for Hastelloy N samples tested in FLiNaK, with and without different metal fluorides, are given in Fig. 12, along with the XRD results for untested Hastelloy N sample for reference. During the baseline test, it can be observed that the Hastelloy N samples show only Ni peaks before and after the exposure test, suggesting that no other compound formed on its surface while exposed to molten salt. Similar results can also be observed for Hastelloy N samples exposed to molten FLiNaK with added CrF₂, FeF₂, FeF₃, and NiF₂ suggesting that there are no intermetallics or compounds formed at the surface. However, there is a large broadening of peaks observed for the sample with added NiF₂ as opposed to the others. In the Hastelloy N samples with added CrF₃, we can also observe peaks corresponding to Cr, suggesting that there is a significant deposition of Cr at the surface of the alloy in this test.

The SEM images and EDS line scans of the cross-sections of Hastelloy N samples exposed to molten FLiNaK with added CrF₂, CrF₃, FeF₂, FeF₃, and NiF₂ are given in Figs. 13–17, respectively. The effect of metal fluoride addition on corrosion of Hastelloy N samples was less dramatic than SS316H samples. However, it can still be observed that the extent of attack, marked by selective leaching of elements like Cr, increases from CrF₂ (5 μm) to CrF₃ (8 μm) to FeF₂ (10 μm) to FeF₃ (14 μm) to NiF₂ (20 μm). The SEM images show that, unlike with the presence of oxides and other impurities reported elsewhere, the addition of metal fluorides does not lead to visible attack or micro-void formation [14,21]. The EDS line scans show evidence of disproportionation reaction at the surface, with various metal fluorides leading to increase in concentration of that metal at the Hastelloy N surface. The presence of CrF₂ and CrF₃, shown in Figs. 13 and 14 respectively, results in the presence of non-uniform Cr-rich regions. This is more apparent in the sample exposed to FLiNaK with added CrF₃ than the one exposed to FLiNaK with added CrF₂. In the sample exposed to FLiNaK with added CrF₂ in Fig. 13 (b), we observed the presence of a thin Cr-rich layer that indicates that disproportionation reaction has occurred with Cr depositing on the

surface. However, in another area of the same sample in Fig. 13 (c), this layer is not observable, with a slight Cr depletion present. Similar effects can be observed at a much larger scale for the sample exposed to FLiNaK with added CrF₃, in Fig. 14 (b) and Fig. 14 (c). The Cr-rich layer is much thicker in this sample, giving clear evidence of deposition of Cr at the surface. However, the leaching of Cr is also higher in the areas where there is no Cr rich layer on the sample surface. The difference in size of these layers might suggest why the sample exposed to FLiNaK with added CrF₃ shows XRD peaks corresponding to Cr while the one exposed to FLiNaK with CrF₂ does not. The non-uniformity of these layers suggests that, despite the mass loss in these samples being lower than the baseline, addition of CrF₂ or CrF₃ will not be a deterrent to corrosion due to the non-uniformity.

The addition of FeF₂ and FeF₃, given in Figs. 15 and 16, lead to an increase in the concentration of Fe and a decrease in concentrations of Cr, Mo etc. at the surface. This effect is higher for FeF₃ than FeF₂, probably due to the more positive energy of formation of FeF₃ that leads to more disproportionation reaction as well as FeF₃ reducing to more FeF₂ than direct addition of FeF₂, by Eq. 2. The addition of NiF₂, given in Fig. 17, leads to an increase in the concentration of Ni at the surface and decrease in the concentration of all other alloying elements, indicating that Ni from NiF₂ is reducing on the surface of Hastelloy N with other alloying elements forming fluorides and undergoing selective leaching. However, unlike with SS316H discussed earlier, and unlike with Hastelloy N exposed to molten FLiNaK with added oxides of similar amount studied previously [21], the presence of metal fluorides in molten FLiNaK does not seem to lead to catastrophic effects in Hastelloy N. This indicates that Hastelloy N as a structural material can withstand the accidental formation of various metal fluorides in the molten salt during FHR or CSP operation, whereas SS316H will be significantly more affected by these impurities.

The concentration of major alloying elements (Cr, Fe, Mo, Ni, and Mn) at the surfaces of the various tested Hastelloy N and SS316H samples are given in Figs. 18 and 19 respectively. The values for Hastelloy N in Fig. 18 show clear evidence of disproportionation reactions at the surface, with samples exposed to FLiNaK with added CrF₂ and CrF₃

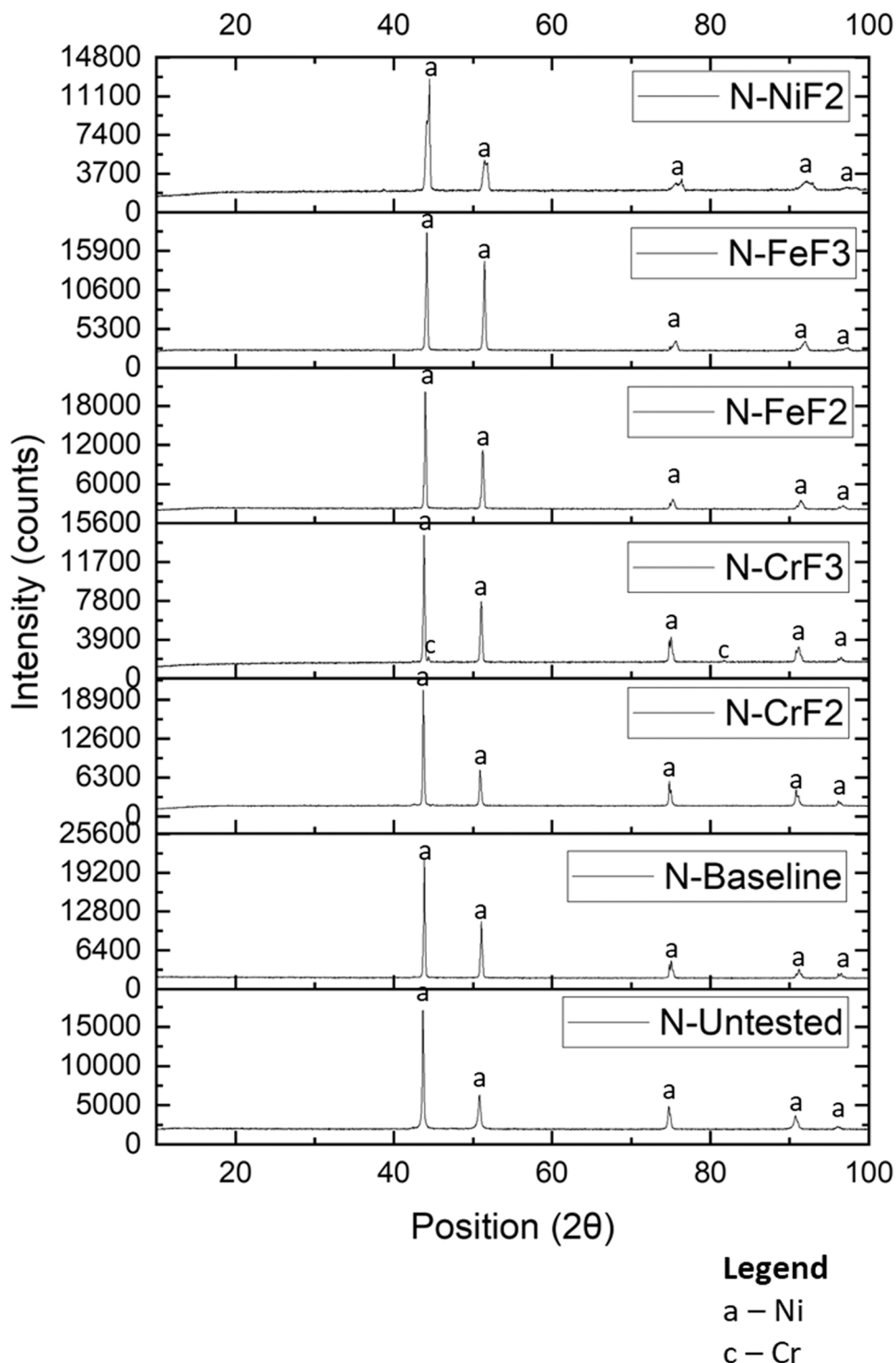


Fig. 12. XRD peaks for Hastelloy N samples before and after being exposed to molten FLiNaK salt with or without added metal fluorides.

showing a peak in Cr concentration at the surface, samples exposed to added FeF_2 and FeF_3 showing a peak in Fe concentration at the surface, and sample exposed to added NiF_2 showing a peak in Ni concentration. Aside from these disproportionation reactions, a general trend of a decrease in concentration of Cr, Fe, and Mo (for less stable fluorides) was also observed, which is due to the selective dissolution of these elements from Hastelloy N surfaces in molten salt [29]. These trends are also noticeable in the SS316H samples in Fig. 19. Even though the SEM-EDS results did not show evidence of disproportionation reactions, enrichment of Cr in samples exposed to added CrF_2 and CrF_3 can be observed.

However, this could also be due to the mode of attack switching from a uniform mode with Cr depletion in the baseline sample to the intergranular mode in the samples with added CrF_2 and CrF_3 . Intergranular attack is not easily detected by XRF as the localized depletion of elements is associated with only the grain boundaries at the surface. Selective leaching of Mn is not shown in Hastelloy N due to the very low initial concentration of Mn in Hastelloy N, but Mn concentration of SS316H also shows a general trend of selective dissolution very similar to Cr, with less attack visible in samples exposed to FLiNaK with added CrF_3 or FeF_2 due to the more intergranular nature of the attack in these

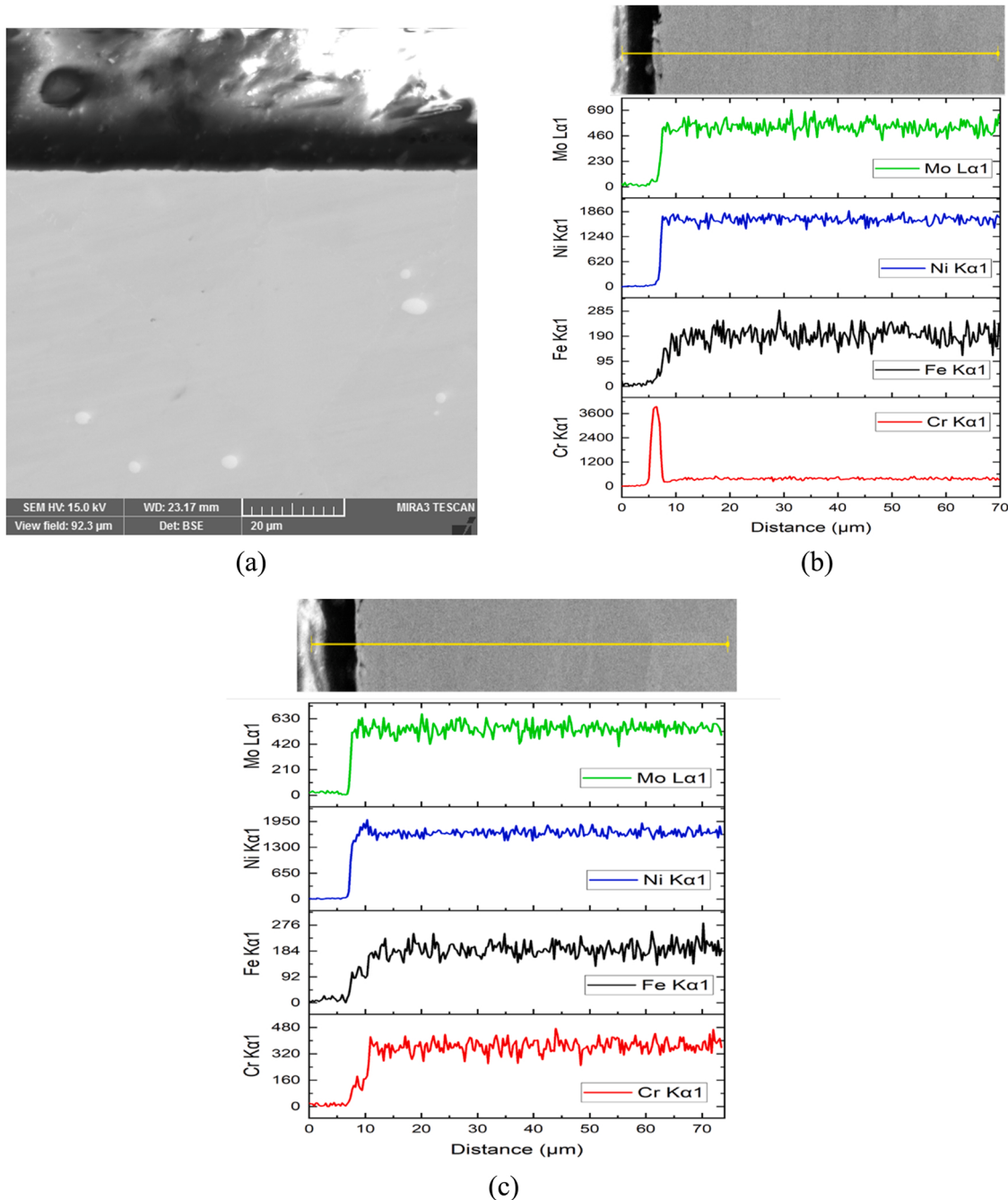


Fig. 13. (a) SEM image and (b)&(c) EDS line scans at various regions of cross-section of Hastelloy N sample exposed to FLiNaK salt with added 0.2 mol% CrF₂.

samples. It can also be observed that the samples which show an increased leaching of Mn are also the specimens that displayed XRD peaks corresponding to ferrite/martensite in Fig. 6. An increase in Ni and Mo concentration at the surface with increased corrosion can also be observed in SS316H samples. This could be due to the selective dissolution of Mn, Cr and Fe reaching critical stages where Ni and Mo appears enriched at the surface, as XRF gives relative abundance of the elements at the surface of the alloy.

As the selective dissolution in 316 H samples in FLiNaK molten salts was also associated with the local phase changes, especially the formation of BCC Ferrite and/or BCT martensite which leads to an increase in the magnetic response of the material [20,23,24], we decided to measure the magnetic response of tested samples. Ferrite Number (FN) of a material is a measure of the ferrite content of the material [30]. Feritscopes was used to determine the FN of materials, which correlates

with the magnetic nature of the material. The FN for certain materials such as pure Iron and Ferritic steels are usually in the order of 100s, while that for Austenitic Stainless steels are usually less than 1, and that for most non-ferrous metals such as Mo, Cr etc. is 0. As such, FN of SS316H is a useful measure of the extent to which the material has undergone corrosion. Nickel based alloys such as Hastelloy N are expected to always have FN of 0, and this can be used as a measure to determine if there is a coating of any ferrous materials on the surface of Hastelloy N. The FN of Hastelloy N and SS316H samples that are untested, and samples tested in FLiNaK as well as FLiNaK with added metal fluorides is given in Fig. 20. The FN of Hastelloy N, given in Fig. 20 (a) show that the untested sample as well as the samples exposed to molten FLiNaK, molten FLiNaK with added CrF₂, added CrF₃, and added NiF₂ all show a FN of zero, as expected from Hastelloy N. However, the Hastelloy N samples exposed to molten FLiNaK with added FeF₂ and FeF₃ show a

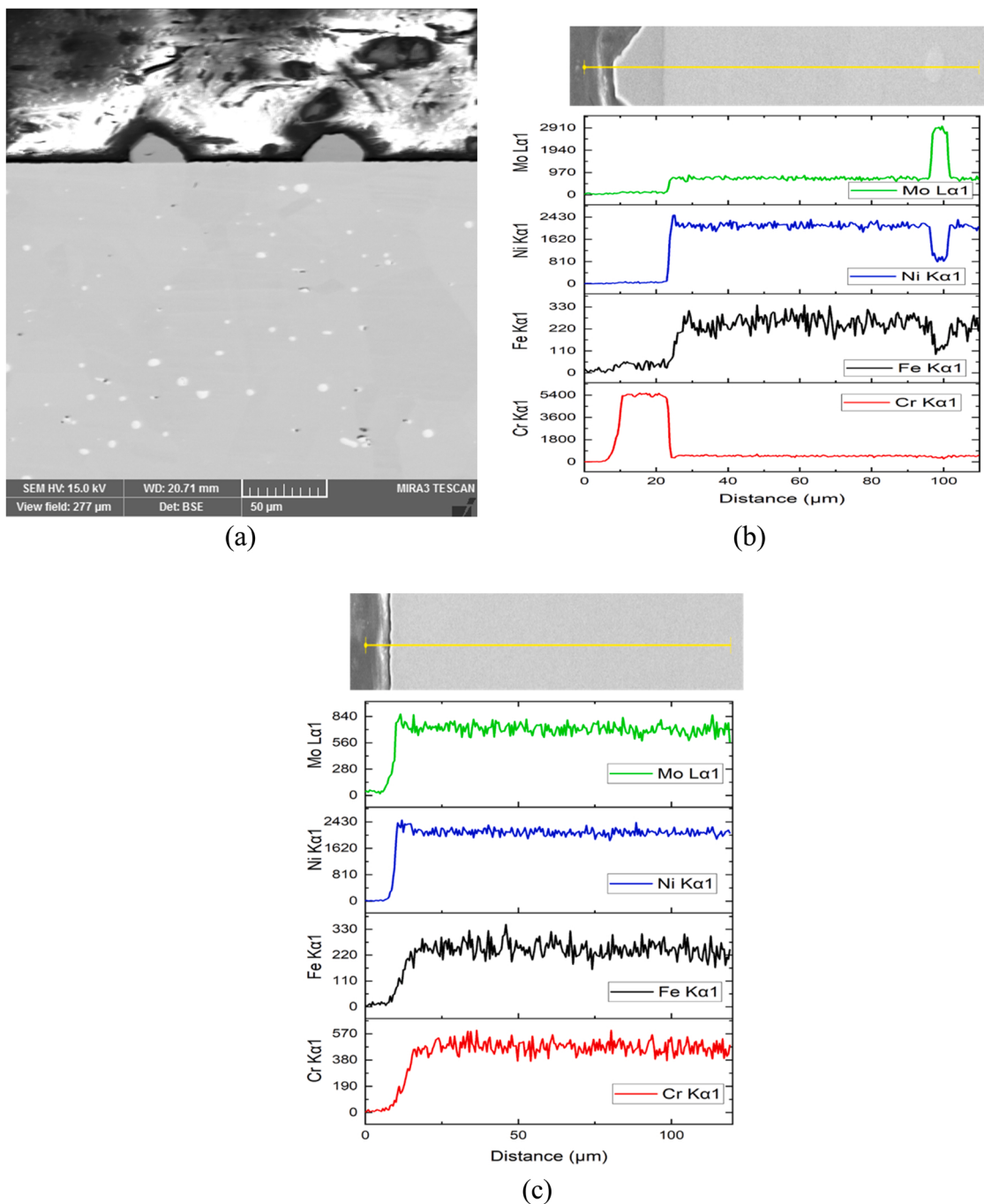


Fig. 14. (a) SEM image and (b)&(c) EDS line scans at various regions of cross-section of Hastelloy N sample exposed to FLiNaK salt with added 0.2 mol% CrF₃.

higher FN, demonstrating that there is presence of Fe (ferrite) on the surface. This confirms the findings of EDS and XRF that there is deposition of iron at the surface of Hastelloy N when exposed to these salts. Similar to what has been observed through SEM and XRF, the FN is higher for the sample exposed to FLiNaK + FeF₃ than the one exposed to FLiNaK + FeF₂. The FN of SS316H, given in Fig. 20 (b) show an increase in FN which corresponds to the increase in extent of corrosion observed in Figs. 7–11. The FN of the untested sample is around 0.4 and the XRD graph for this sample in Fig. 6 show only austenite peaks. The sample exposed to molten FLiNaK, which had XRD peaks corresponding to both Austenite and Ferrite, has a FN of around 0.75. This confirms that the exposure to molten FLiNaK salt increases the tendency of Austenite to transform to Ferrite. The FN of SS316H increases with the more positive metal fluorides added and can be correlated to the extent of corrosion of

these samples, indicated in Fig. 4. It has to be noted that the samples which did not show ferrite/martensite peak in XRD, such as the SS316H samples exposed to FLiNaK with added CrF₃ or FeF₂ also show a higher FN than the untested or baseline samples. These samples typically had an intergranular attack, and the selective dissolution was mostly concentrated along the grain boundaries. This change could be detected by the change in the magnetic behavior of samples as the FN can be detected at a further depth than XRD, which is a more surface level technique which did not pick this localized phase change. This also confirms the findings of our previous work that FN can be a useful measure of the extent of corrosion of SS316H in molten salts, as the higher FN values indicate a higher extent of corrosion [20].

From these results, it becomes clear that the presence of metal fluorides can have a significant effect on the corrosion of structural alloy

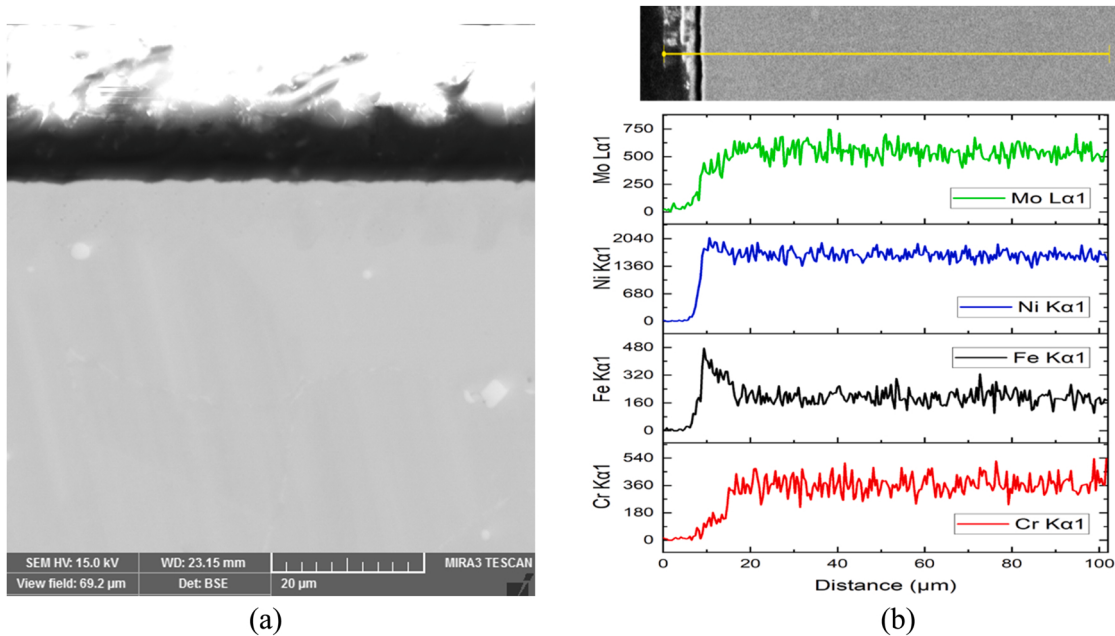


Fig. 15. (a) SEM image and (b) EDS line scan of cross-section of Hastelloy N sample exposed to FLiNaK salt with added 0.2 mol% FeF₂.

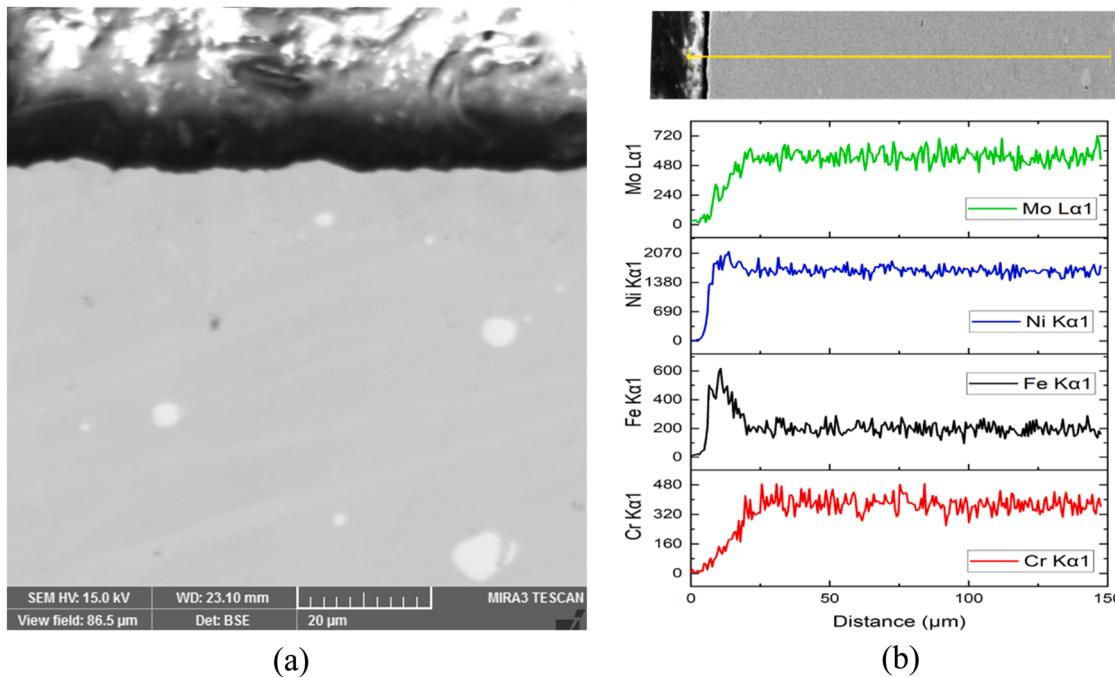


Fig. 16. (a) SEM image and (b) EDS line scan of cross-section of Hastelloy N sample exposed to FLiNaK salt with added 0.2 mol% FeF₃.

in molten FLiNaK salt, depending on the alloy used. The SS316H samples underwent drastically increasing intergranular attack in the presence of less stable metal fluorides which can still form in FHR and CSP conditions. The Hastelloy N samples showed a much less extent of attack, but the formation of disproportionation reaction products on the surface of these samples is a cause of concern as their properties, including mechanical properties and interactions with other impurities, graphite, fission products etc. are not known. The increased attack on SS316H is also concerning because SS316H is code-certified by ASME for application in high temperature reactors, whereas Hastelloy N is not code-certified for these applications at FHR temperatures of above 650 °C [31]. Due to this, most commercial designs of MSRs and CSPs involve the

application of Austenitic Stainless Steels such as 316H [32]. As such, this study shows that it is important to control the presence of these impurities in molten fluoride salts.

4. Conclusion

In this work, the effect of presence of various metal fluorides on the corrosion of Hastelloy N and SS316H in molten FLiNaK salt was studied. Based on the results, the conclusions are:

- The presence of metal fluorides results in an increase in the corrosion of structural alloy. The extent of increase in corrosion is determined

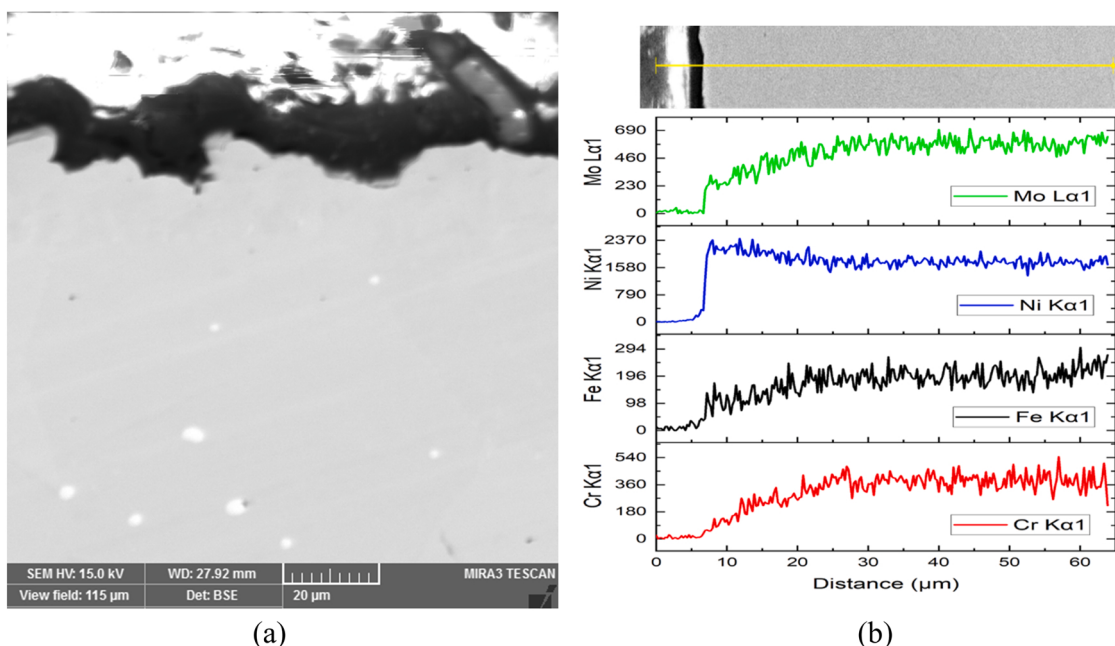


Fig. 17. (a) SEM image and (b) EDS line scan of cross-section of Hastelloy N sample exposed to FLiNaK salt with added 0.2 mol% NiF₂.

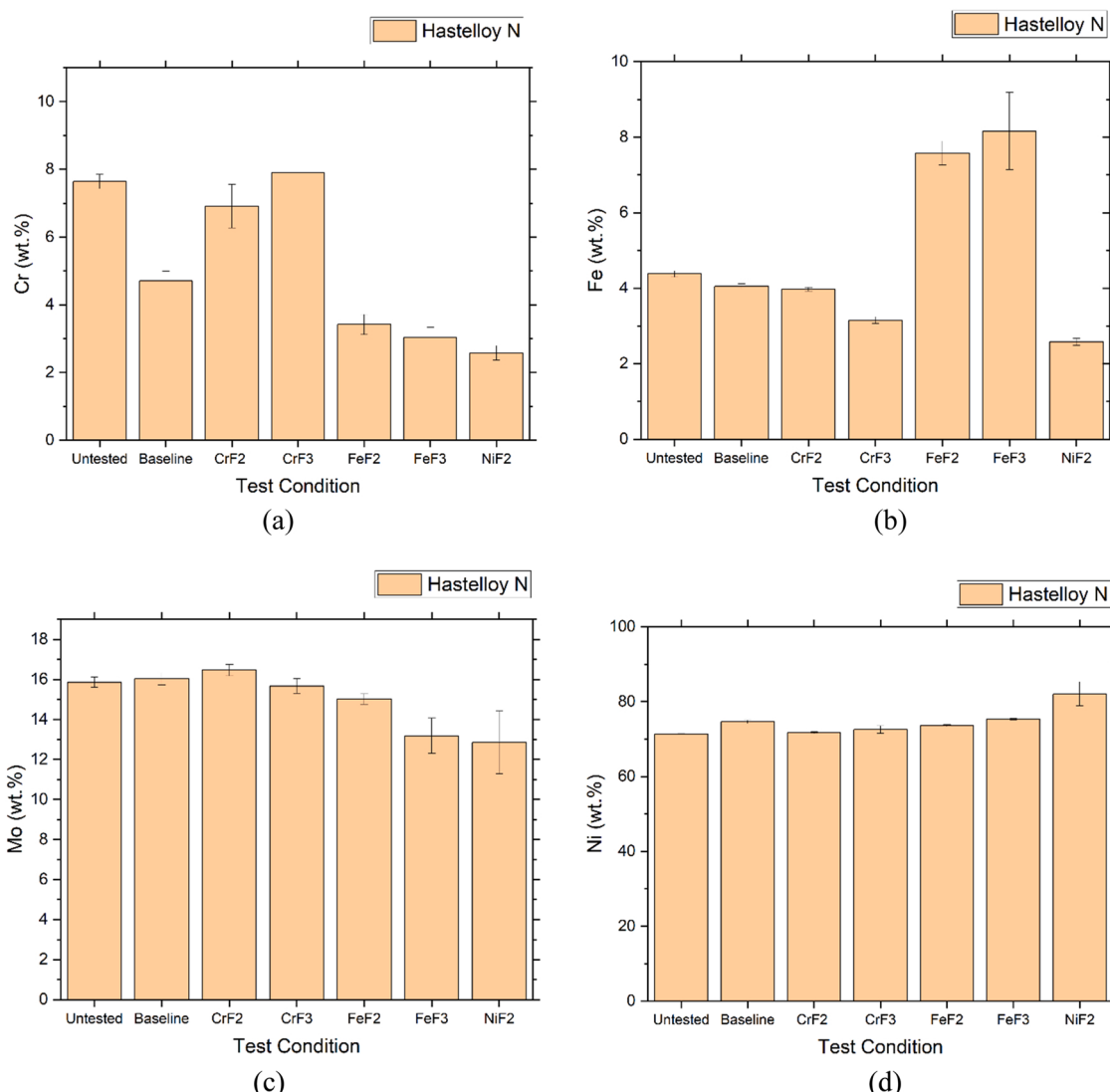


Fig. 18. XRF results showing (a) Cr content, (b) Fe content, (c) Mo content, and (d) Ni content at the surfaces of Hastelloy N samples before and after being exposed to molten FLiNaK salt with or without added metal fluorides.

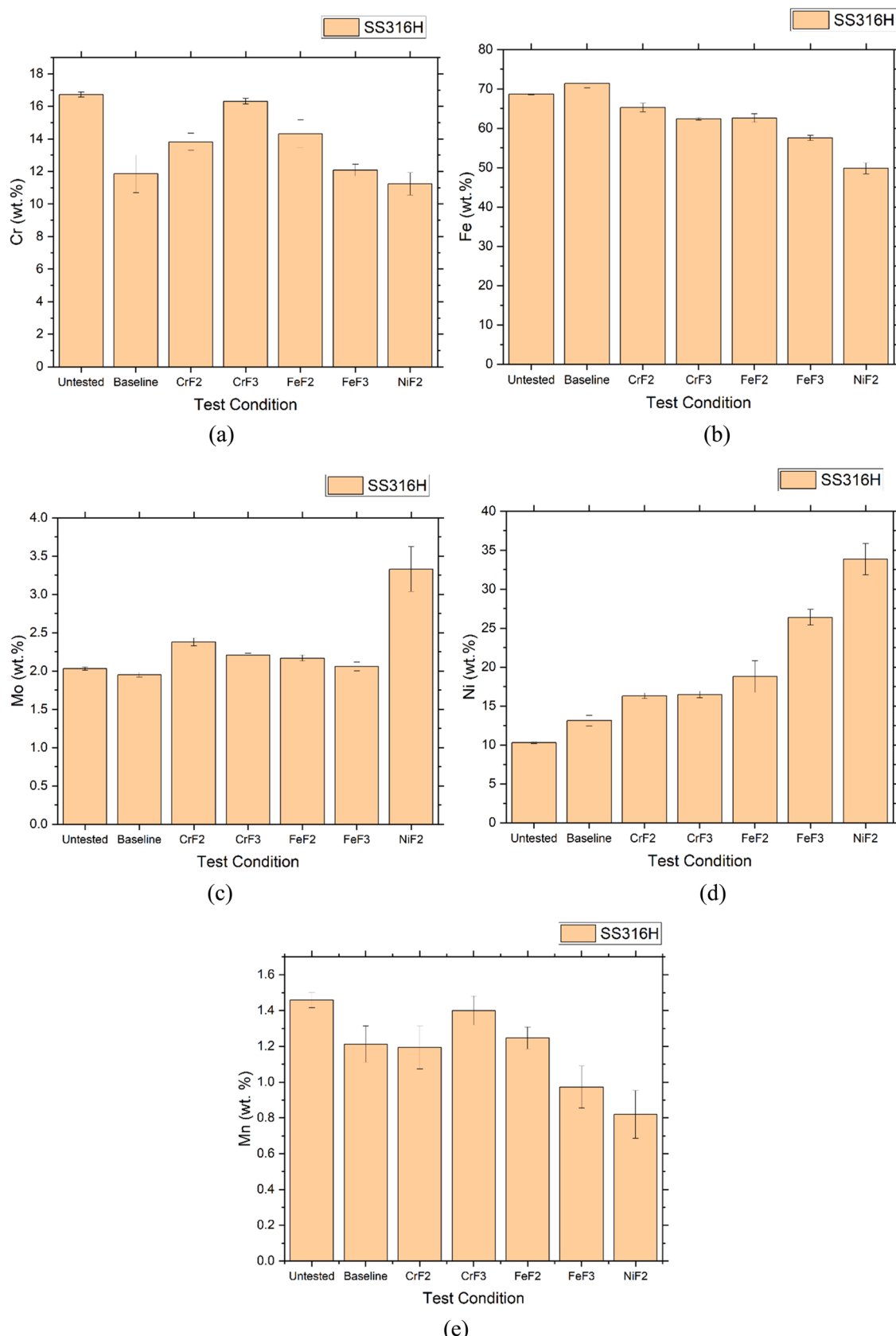


Fig. 19. XRF results showing (a) Cr content, (b) Fe content, (c) Mo content, (d) Ni content, and (e) Mn content at the surfaces of SS316H samples before and after being exposed to molten FLiNaK salt with or without added metal fluorides.

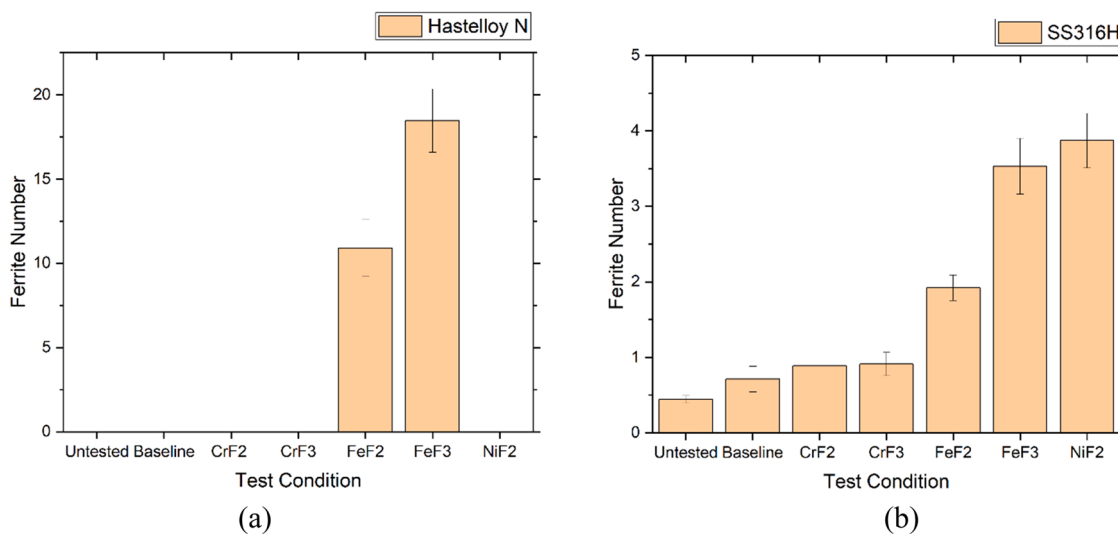


Fig. 20. Ferrite Number (FN) values for (a) Hastelloy N and (b) SS316H samples before and after being exposed to molten FLiNaK salt with or without added metal fluorides.

by both the thermodynamic stability of the metal fluoride impurity added as well as the composition of the structural alloy studied.

- The relative effect of added impurities on the extent of corrosion in both Hastelloy N and SS316H samples were: Baseline < CrF₂ < CrF₃ < FeF₂ < FeF₃ < NiF₂. This matches with previous findings of Pavlík et al. [13] for Incoloy 800 H, suggesting that different types of alloys behave in similar manner in presence of FLiNaK with metal fluorides, with the main difference being the extent of change in degradation.
- The SS316H samples had a significant increase in the depth of intergranular attack in the presence of less stable metal fluorides. SS316H samples tested in FLiNaK with addition of FeF₂, FeF₃, and NiF₂ showed a K₂NaCrF₆ layer at the sample surface.
- Hastelloy N showed an increased corrosion with addition of tested metal fluoride impurities. However, for Hastelloy N samples, corrosion was relatively smaller than for SS316H samples.
- There is clear evidence of disproportionation reaction on the surface of Hastelloy N samples exposed to molten FLiNaK with added metal fluorides of Cr and Fe.
- The presence of metal fluoride impurities in molten FLiNaK salt is detrimental to the corrosion behavior of tested structural alloys. Results show that if the less-stable metal fluorides such as NiF₂ or FeF₃ are present in the molten salt system, then the 316 H stainless steel may see a significant increase in corrosion depending on the amount of these impurities present.

CRediT authorship contribution statement

Krishna Moorthi Sankar: Investigation, Experiments, Data Analysis, Writing – original draft. **Preet M Singh:** Supervision, Methodology, Data Analysis, Writing – review & editing.

Declaration of Competing Interest

The authors declare that they have no known competing financial interests or personal relationships that could have appeared to influence the work reported in this paper.

Data availability

Data will be made available on request.

Acknowledgments

This work was supported by the U.S. Department of Energy Nuclear Energy University Program (DOE-NEUP) under Award DE-NE0008749. Any opinions, conclusions, findings, or recommendations in this publication are those of the authors and do not necessarily reflect the views of the Department of Energy Office of Nuclear Energy. The authors wish to acknowledge Vikhyat Arun, from Chattahoochee High School, Johns Creek, GA, for his help with data collection for this project.

References

- [1] Manohar S. Sohal, Matthias A. Ebner, Piyush Sabharwall, Phil Sharpe, Engineering database of liquid salt thermophysical and thermochemical properties, 2010. <https://doi.org/10.2172/980801>.
- [2] T. Bauer, C. Odenthal, A. Bonk, Molten salt storage for power generation, Chem. Ing. Tech. 93 (2021) 534–546, <https://doi.org/10.1002/cite.202000137>.
- [3] J. Serp, M. Alibert, O. Benes, S. Delpech, O. Feynberg, V. Ghetta, D. Heuer, D. Holcomb, V. Ignatiev, J.L. Kloosterman, L. Luzzi, E. Merle-Lucotte, J. Uhlfir, R. Yoshioka, D. Zhimin, The molten salt reactor (MSR) in generation IV: overview and perspectives, Prog. Nucl. Energy 77 (2014) 308–319, <https://doi.org/10.1016/j.pnucene.2014.02.014>.
- [4] P.M. Singh, K.J. Chan, C.S. Deo, V. Deodeshmukh, J.R. Keiser, W. Ren, T.L. Sham, D.F. Wilson, G. Yoder, J. Zhang, Phenomena Identification and ranking table (PIRT) study for metallic structural materials for advanced high-temperature reactor, Ann. Nucl. Energy 123 (2019) 222–229, <https://doi.org/10.1016/j.anucene.2018.08.036>.
- [5] J. Zhang, C.W. Forsberg, M.F. Simpson, S. Guo, S.T. Lam, R.O. Scarlat, F. Carotti, K. J. Chan, P.M. Singh, W. Doniger, K. Sridharan, J.R. Keiser, Redox potential control in molten salt systems for corrosion mitigation, Corros. Sci. 144 (2018) 44–53, <https://doi.org/10.1016/j.corsci.2018.08.035>.
- [6] K. Hansson, K.M. Sankar, P.F. Weck, J.K. Startt, R. Dingreville, C.S. Deo, J.D. Sugar, P.M. Singh, Effect of excess Mg to control corrosion in molten MgCl₂ and KCl eutectic salt mixture, Corros. Sci. 194 (2022), 109914, <https://doi.org/10.1016/j.corsci.2021.109914>.
- [7] X.-X. Ye, H. Ai, Z. Guo, H. Huang, L. Jiang, J. Wang, Z. Li, X. Zhou, The high-temperature corrosion of Hastelloy N alloy (UNS N10003) in molten fluoride salts analysed by STXM, XAS, XRD, SEM, EPMA, TEM/EDS, Corros. Sci. 106 (2016) 249–259, <https://doi.org/10.1016/j.corsci.2016.02.010>.
- [8] S.S. Raiman, S. Lee, Aggregation and data analysis of corrosion studies in molten chloride and fluoride salts, J. Nucl. Mater. 511 (2018) 523–535, <https://doi.org/10.1016/j.jnucmat.2018.07.036>.
- [9] J. Ambrosek, M. Anderson, K. Sridharan, T. Allen, Current status of knowledge of the fluoride salt (FLiNaK) heat transfer, Nucl. Technol. 165 (2009) 166–173, <https://doi.org/10.13182/NT165-166>.
- [10] L.C. Olson, J.W. Ambrosek, K. Sridharan, M.H. Anderson, T.R. Allen, Materials corrosion in molten LiF-NaF-KF salt, J. Fluor. Chem. 130 (2009) 67–73, <https://doi.org/10.1016/j.fluchem.2008.05.008>.
- [11] F.-Y. Ouyang, C.-H. Chang, B.-C. You, T.-K. Yeh, J.-J. Kai, Effect of moisture on corrosion of Ni-based alloys in molten alkali fluoride FLiNaK salt environments, J. Nucl. Mater. 437 (2013) 201–207, <https://doi.org/10.1016/j.jnucmat.2013.02.021>.

- [12] E. Karfidow, E. Nikitina, M. Erzhenkov, K. Seliverstov, P. Cherneky, A. Mullabaev, V. Tsvetov, P. Mushnikov, K. Karimov, N. Molchanova, A. Kuznetsova, Corrosion behavior of candidate functional materials for molten salts reactors in LiF-NaF-KF containing actinide fluoride imitators, Materials 15 (2022) 761, <https://doi.org/10.3390/ma15030761>.
- [13] V. Pavlák, M. Kontrík, M. Boča, Corrosion behavior of Incoloy 800H/HT in the fluoride molten salt FLiNaK + MF_x (MF_x = CrF₃, FeF₂, FeF₃ and NiF₂), N. J. Chem. 39 (2015) 9841–9847, <https://doi.org/10.1039/C5NJ01839K>.
- [14] Y.L. Wang, Q. Wang, H.J. Liu, C.L. Zeng, Effects of the oxidants H₂O and CrF₃ on the corrosion of pure metals in molten (Li,Na,K)F, Corros. Sci. 103 (2016) 268–282, <https://doi.org/10.1016/j.corsci.2015.11.032>.
- [15] H. Yin, J. Qiu, H. Liu, W. Liu, Y. Wang, Z. Fei, S. Zhao, X. An, J. Cheng, T. Chen, P. Zhang, G. Yu, L. Xie, Effect of CrF₃ on the corrosion behaviour of Hastelloy-N and 316L stainless steel alloys in FLiNaK molten salt, Corros. Sci. 131 (2018) 355–364, <https://doi.org/10.1016/j.corsci.2017.12.008>.
- [16] W.H. Doniger, C. Falconer, M. Elbakshwan, K. Britsch, A. Couet, K. Sridharan, Investigation of impurity driven corrosion behavior in molten 2LiF-BeF₂ salt, Corros. Sci. 174 (2020), 108823, <https://doi.org/10.1016/j.corsci.2020.108823>.
- [17] H. Ai, Y. Liu, M. Shen, H. Liu, Y. Chen, X. Yang, H. Liu, Y. Qian, J. Wang, Dissolved valence state of iron fluorides and their effect on Ni-based alloy in FLiNaK salt, Corros. Sci. 192 (2021), 109794, <https://doi.org/10.1016/j.corsci.2021.109794>.
- [18] J.W. Koger, Effect of FeF₂ addition on mass transfer in a hastelloy N - LiF-BeF₂-UF₄ thermal convection loop system, ORNL-TM 4188 (1972).
- [19] M. Weinstein, C. Falconer, W. Doniger, L. Bailly-Salins, R. David, K. Sridharan, A. Couet, Environmental degradation of electroplated nickel and copper coated SS316H in molten FLiNaK salt, Corros. Sci. 191 (2021), 109735, <https://doi.org/10.1016/j.corsci.2021.109735>.
- [20] K.M. Sankar, P.M. Singh, Effect of Li metal addition on corrosion control of Hastelloy N and stainless steel 316H in molten LiF-NaF-KF, J. Nucl. Mater. 555 (2021), 153098, <https://doi.org/10.1016/j.jnucmat.2021.153098>.
- [21] K.M. Sankar, P.M. Singh, Effect of oxide impurities on the corrosion behavior of structural materials in molten LiF-NaF-KF, Corros. Sci. 206 (2022), 110473, <https://doi.org/10.1016/j.corsci.2022.110473>.
- [22] G. Zheng, B. Kelleher, G. Cao, M. Anderson, T. Allen, K. Sridharan, Corrosion of 316 stainless steel in high temperature molten Li₂BeF₄ (FLiBe) salt, J. Nucl. Mater. 461 (2015) 143–150, <https://doi.org/10.1016/j.jnucmat.2015.03.004>.
- [23] K.J. Chan, Carbon Effects on Corrosion in Molten Fluoride Salt (Ph.D. Thesis), Georgia Institute of Technology,, 2020.
- [24] E.P. Butler, M.G. Burke, Chromium depletion and martensite formation at grain boundaries in sensitised austenitic stainless steel, Acta Metall. 34 (1986) 557–570, [https://doi.org/10.1016/0001-6160\(86\)90091-X](https://doi.org/10.1016/0001-6160(86)90091-X).
- [25] K. Knox, The preparation and structure of K₂NaCrF₆, K₂NaFeF₆, and K₂NaGaF₆, J. Inorg. Nucl. Chem. 21 (1961) 253–258.
- [26] R.S. Sellers, M.H. Anderson, K. Sridharan, T.R. Allen, Failure analysis of 316L stainless steel crucible by molten fluoride salt interaction with clay bonded silicon carbide, Eng. Fail. Anal. 42 (2014) 38–44, <https://doi.org/10.1016/j.englfailanal.2014.03.007>.
- [27] R.S. Sellers, Impact of Reduction-oxidation Agents on the High Temperature Corrosion of Materials in LiF-NAF-KF (MS Thesis), University of Wisconsin, Madison, 2012.
- [28] A. Thompson, A Study of Stainless Steel as a Material of Construction for a Molten Salt Reactor. (Ph.D. thesis), University of Sheffield, 2019.
- [29] Sylvie Delpech, C. Cabet, C. Slim, G.S. Picard, Molten fluorides for nuclear applications, Mater. Today 13 (2010) 34–41, [https://doi.org/10.1016/S1369-7021\(10\)70222-4](https://doi.org/10.1016/S1369-7021(10)70222-4).
- [30] J.C.M. Farrar, The measurement of ferrite number (FN) in real weldments — Final Report, Weld. World 49 (2005) 13–21, <https://doi.org/10.1007/BF03263405>.
- [31] K. Fukumoto, R. Fujimura, M. Yamawaki, Y. Arita, Corrosion behavior of Hastelloy-N alloys in molten salt fluoride in Ar gas or in air, J. Nucl. Sci. Technol. 52 (2015) 1323–1327, <https://doi.org/10.1080/00223131.2015.1043155>.
- [32] B. Barua, M. Messner, T.-L. Sham, R. Jetter, Y. Wang, S. Huang, G. Young, Design rules for 316H nuclear components cladded with nickel or tungsten, 2021. <https://doi.org/10.2172/1772469>.